Journal of Biomedical Optics

BiomedicalOptics.SPIEDigitalLibrary.org

Characteristics of laser-induced shock wave injury to the inner ear of rats

Takaomi Kurioka
Takeshi Matsunobu
Katsuki Niwa
Atsushi Tamura
Satoko Kawauchi
Yasushi Satoh
Shunichi Sato
Akihiro Shiotani

SPIE.

Characteristics of laser-induced shock wave injury to the inner ear of rats

Takaomi Kurioka,[a] Takeshi Matsunobu,[a,*] Katsuki Niwa,[a] Atsushi Tamura,[a] Satoko Kawauchi,[b] Yasushi Satoh,[c] Shunichi Sato,[b] and Akihiro Shiotani[a]
[a]National Defense Medical College, Department of Otolaryngology-Head and Neck Surgery, 3-2 Namiki, Tokorozawa, Saitama 359-8513, Japan
[b]National Defense Medical College Research Institute, Division of Biomedical Information Sciences, 3-2 Namiki, Tokorozawa, Saitama 359-8513, Japan
[c]National Defense Medical College, Department of Anesthesiology, 3-2 Namiki, Tokorozawa, Saitama 359-8513, Japan

Abstract. Recently, the number of blast injuries of the inner ear has increased in the general population. In blast-induced inner ear injury, a shock wave (SW) component in the blast wave is considered to play an important role in sensorineural hearing loss. However, the mechanisms by which an SW affects inner ear tissue remain largely unknown. We aimed to establish a new animal model for SW-induced inner ear injury by using laser-induced SWs (LISWs) on rats. The LISWs were generated by irradiating an elastic laser target with 694-nm nanosecond pulses of a ruby laser. After LISW application to the cochlea through bone conduction, auditory measurements revealed the presence of inner ear dysfunction, the extent of which depended on LISW overpressure. A significantly lower survival rate of hair cells and spiral ganglion neurons, as well as severe oxidative damage, were observed in the inner ear exposed to an LISW. Although considerable differences in the pressure characteristics exist between LISWs and SWs in real blast waves, the functional and morphological changes shown by the present LISW-based model were similar to those observed in real blast-induced injury. Thus, our animal model is expected to be useful for laboratory-based research of blast-induced inner ear injury. [DOI: 10.1117/1.JBO.19.12.125001]

Keywords: blast injury; laser-induced shock waves; inner ear; sensorineural hearing loss.

Paper 140420RR received Jul. 7, 2014; accepted for publication Nov. 3, 2014; published online Dec. 2, 2014.

1 Introduction

Exposure to blast overpressure has become one of the most serious hazards in both military and civilian life worldwide because of war and terrorist activities. Although auditory damage is one of the primary sequelae of blast injury, it has yet to be determined how a blast wave is transmitted to the inner ear, affects its biological functioning, and causes damage at the cellular level. Therefore, comprehensive research is required for the prevention, diagnosis, and treatment of blast-induced hearing loss. However, at present, it is difficult to model precise clinical and mechanical complexities resulting from blast-induced inner ear injuries under laboratory conditions. Out of all the components in a blast wave, a shock wave (SW) is considered to play an important role because it is the most invasive component with an extremely fast rise and high peak in pressure. However, a reliable animal model of SW-induced inner ear injury has yet to be established. Consequently, the mechanisms by which an SW affects inner ear tissue remain largely unknown.

The irradiation of a solid material with a high-power laser pulse induces an SW through the expansion of the laser-induced plasma. This phenomenon is termed as a laser-induced SW (LISW), a laser-induced stress wave, or a photomechanical wave. Over the last 10 years, LISWs have been used to deliver drug molecules or genes to tissue *in vivo*, creating a new regime of laser photonic therapy.[1–3] However, we found that the excessive increases in LISW pressure caused tissue damage, which inspired us to employ LISWs to study SW-induced injuries. The advantages of using LISWs for studying SW-induced injuries include safety, ease of use, and compactness of the generating device, as well as highly versatile and controllable SW energy, both spatially and temporally. Furthermore, LISW-induced injuries may be observed in selectively exposed tissue regions, allowing the study of isolated injuries without concomitant injuries. These characteristics facilitate the implementation of many unique animal experiments that cannot be performed with other SW sources. For instance, LISWs have recently been used to study SW-induced pulmonary injuries and brain injuries in rodents.[4,5]

In this study, we applied LISW to the cochlea through the postauricular temporal bone of the rat and carefully examined the auditory brainstem response (ABR), the loss of outer hair cells (OHCs) and spiral ganglion neurons (SGNs), and oxidative DNA damage in the inner ear. Furthermore, this study set out to validate that our LISW animal models could be used to simulate SW-induced inner ear injuries under real blast wave situations through comparison of physiological and microscopic characteristics, despite the two wave types having considerable differences in pressure characteristics.

2 Materials and Methods

2.1 *Animals*

Five-week-old male Sprague-Dawley rats weighing 150 to 200 g with a normal Preyer's reflex were obtained from Japan SLC, Inc. (Shizuoka, Japan) for use in this study. The

*Address all correspondence to: Takeshi Matsunobu, E-mail: takeshim@ndmc.ac.jp

0091-3286/2014/$25.00 © 2014 SPIE

animals were given free access to water and were fed a regular diet. All experimental protocols were performed in accordance with the guidelines for animal experiments of the National Defense Medical College and the laws and notifications of the government of Japan.

2.2 *Experimental Settings*

LISWs were generated by irradiating a target, an 8.0-mm diameter, 0.5-mm thick black natural rubber disk bonded with a 1.0-mm-thick transparent polyethylene terephthalate sheet, with a laser pulse from a 694-nm Q-switched ruby laser (Model IB101, NIIC; pulse width, 20 ns), as shown in Fig. 1(a). The spot diameter on the target was kept constant at approximately 4 mm × 6 mm. We measured the pressure characteristics of LISWs as a function of laser fluence by using a hydrophone, as shown in Figs. 1(b) and 1(d). The frequency spectra (resulting from fast Fourier transform analysis) are also shown in Fig. 1(c). The waveforms were characterized by a fast rise time, high peak pressure, and short duration. The LISWs have high controllability of SW energy; peak pressure and impulse linearly increase with increasing laser fluence, as shown in Fig. 1(d). In addition, the size of the wave source may be easily changed by changing the laser spot size on the target. The rats were anesthetized by an intraperitoneal (i.p.) injection of ketamine (50 mg/kg) and medetomidine (1.0 mg/kg). A single LISW pulse was applied to the cochlea through the postauricular temporal bone percutaneously, not via external auditory canal (EAC), as shown in Figs. 2(a) and 2(b). By this method, the pinna was pulled forward and, thus, the EAC was closed by the pinna, as shown in Fig. 2(c). Therefore, LISWs hardly reached the inner ear via EAC, and we assumed that this pressure level was too low to induce noise-induced hearing loss. The rats were randomly divided into three groups according to laser fluence. Rats in Groups 1, 2, and 3 ($n = 10$, 10, and 12, respectively) received a low-overpressure SW (5.2 J/cm^2), a middle-overpressure SW (5.6 J/cm^2), and a high-overpressure SW (6.1 J/cm^2), respectively.

2.3 *Assessment of Direct Mechanical Cochlear Damage*

The animals were transcardially perfused with a fixation solution containing 4% paraformaldehyde (PFA) after LISW exposure and decapitated. The entire cochleae were dissected and kept in the fixative overnight. After decalcification with 0.1 M ethylenediaminetetraacetic acid (EDTA) in phosphate-buffered saline (PBS) for 10 days at 4°C, the cochleae were embedded in Tissue-Tek O.T.C. The specimens were prepared as 10-μm-thick cryostat sections, stained with hematoxylin-eosin, and viewed under a light microscope (BX51, Olympus, Japan).

2.4 *Auditory Brainstem Response*

ABR was measured using a single recorder (Synax 1200, NEC, Tokyo, Japan) before, immediately after, and 1, 2, 3, and 4 weeks after LISW exposure, as shown in Fig. 2(e). All the following steps were performed under general anesthesia (i.p. injection of 50 mg/kg ketamine and 1.0 mg/kg medetomidine). After anesthesia, stainless needle electrodes were placed subcutaneously at the vertex and ventrolateral sites of the left and right ears to record the response to sound stimuli. Tone burst stimuli (0.2 msrise/fall time and 1 ms flat segment at frequencies of 4, 8, 12, 16, 20, and 32 kHz) were generated.

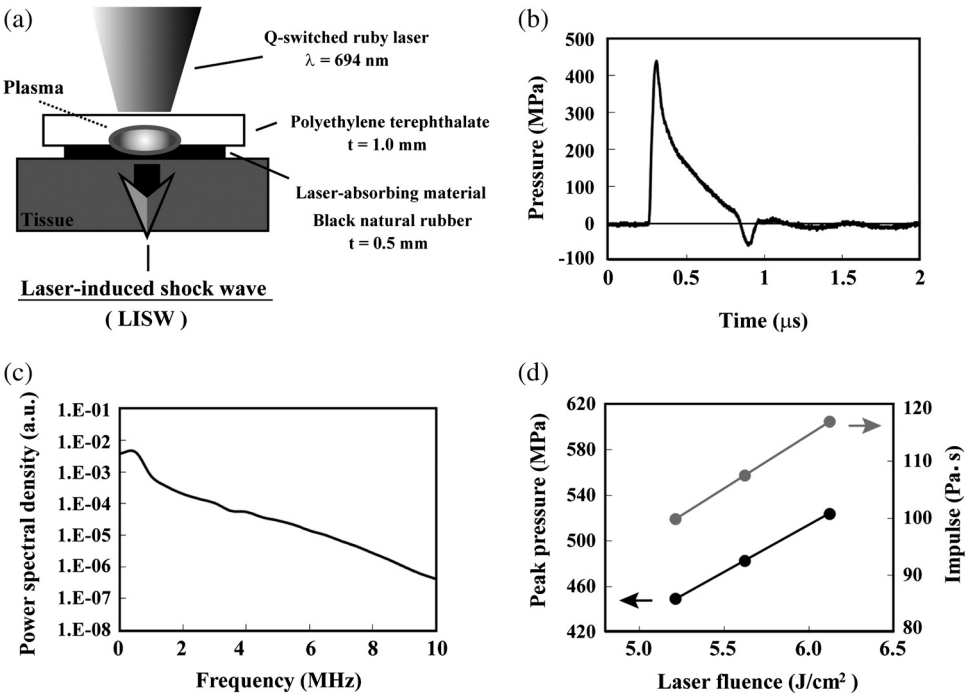

Fig. 1 (a) Experimental setup for the animal model of inner ear blast injury by using laser-induced shock waves (LISWs). The LISWs were generated through the irradiation of a laser target (black rubber) with a Q-switched ruby laser. Plasma formation occurred at the interface between a transparent material and the black rubber. Pressure characteristics of LISWs: (b) Waveform (5.2 J/cm^2), (c) Frequency spectra (5.2 J/cm^2), and (d) Dependence of peak pressure and impulse on laser fluence. Waveforms and frequency spectrum at 5.6 and 6.1 J/cm^2 were similar to those at 5.2 J/cm^2.

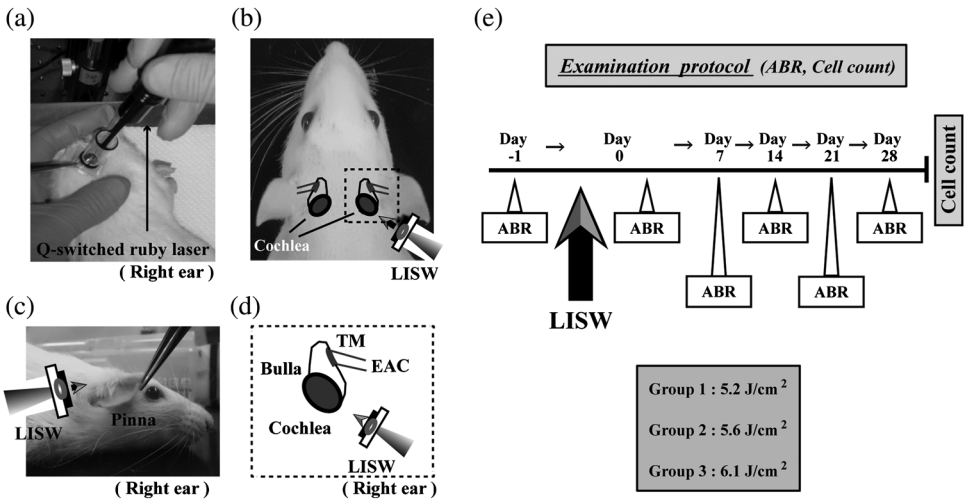

Fig. 2 (a) Image showing how to apply an LISW to induce inner ear injuries. (b) An LISW was applied to the cochlea through the postauricular temporal bone percutaneously. (c) The right pinna was pulled forward, resulting in the closure of the external auditory canal (EAC). (d) Schematic image of LISW application to the cochlea. TM, tympanic membrane. (e) Schedule of the experimental procedures.

The amplitudes were specified by a sound generator and attenuated by a real-time processor and programmable attenuator (RP2.1 and PA5; Tucker-Davis Technologies, Alachua, Florida). The sound stimuli were produced by a coupler-type speaker (ES1spc; Bio Research Center, Nagoya, Japan). The ABR waveforms were recorded for 12.8 ms at a sampling rate of 40,000 Hz by using 50 to 5000 Hz band-pass filter settings. Subsequently, waveforms from 256 stimuli at a frequency of 9 Hz were averaged. The ABR waveforms were recorded at 10 dB sound pressure level intervals down from the maximum amplitude, until no waveform could be visualized. All data values for the ABR thresholds in the text and figures represent the mean ± standard error (SE).

2.5 *Quantitative Assessment of Outer Hair Cell Loss*

Fifteen rats were separated into Group 1 (5.2 J/cm^2, $n = 5$), Group 2 (5.6 J/cm^2, $n = 5$), and Group 3 (6.1 J/cm^2, $n = 5$) and were decapitated 4 weeks after LISW exposure, as shown in Fig. 2(e). The bone near the apex was removed and both the round and oval windows (RW and OW, respectively) were opened, followed by gentle local perfusion with 2×1 mL 4% PFA in 0.1 M PBS (pH 7.4). The tissues were kept in the fixative overnight. The cochleae were dissected by removing the lateral wall bones, lateral wall tissues, and tectorial membranes. After several washings with PBS, the remaining parts of the cochleae were incubated in 0.3% Triton X-100 in PBS for 5 min and washed for an additional three times with PBS. The organs of Corti were stained for F-actin with 1% rhodamine-phalloidin (Invitrogen, Carlsbad, California) for 60 min to outline the hair cells and their stereocilia for quantitative assessment. After several washings with PBS, the organs of Corti were dissected and mounted for surface preparation. The tissues were observed under a confocal fluorescence microscope with a Nikon C1 system (Nikon, Tokyo, Japan) and under a fluorescence microscope (Axio Imager A1; Carl Zeiss MicroImaging Gmbh, Jena, Germany). Then, the number of the missing OHCs in the basal, middle, and apical turns was counted. The ratio of missing OHCs to whole OHCs was expressed as a percentage.

2.6 *Immunohistochemical Analysis of 8-hydroxy-2′-deoxyguanosine*

All animals were deeply anesthetized and killed 5 h after LISW exposure. The bone near the apex was removed, and both the RW and OW were opened, followed by gentle local perfusion with 2×1 mL of 4% PFA. The tissues were preserved overnight in the fixative. The cochleae were dissected by removing the lateral wall bone, lateral wall tissues, and tectorial membranes. After washing with PBS, the remaining parts of the cochlea were incubated in 0.3% Triton X-100 in PBS for 15 min, washed three times, and incubated in a blocking solution of 0.25% casein in PBS (Dako, Glostup, Denmark) to block nonspecific reactions. To detect the oxidative DNA damage, immunolabeling was conducted overnight at 4°C with the mouse monoclonal antibody for 8-hydroxy-2′-deoxyguanosine (8-OHdG) (Nikken Seil Corporation, Shizuoka, Japan) diluted 1:10 in antibody diluent. The sections were washed three times in PBS and incubated with a secondary antibody (Alexa Fluor 488, IgG; Invitrogen) diluted 1:200 in antibody diluent. The specimens were then stained for F-actin with DAPI (4′,6-diamidio-2-phenylindole; Invitrogen), which is a blue fluorescent stain that binds strongly to DNA, at 1:10 in 0.1 M PBS for 15 min at room temperature under protection from light. DAPI labeling was used to identify condensed hair cell nuclei. After rinsing in PBS, the organs of Corti were mounted on slides containing an antifade medium (VECTASHIELD; Vector laboratories, Burlingame, California). Images of the immunolabeled specimens (40× magnification) were taken using a confocal fluorescence microscope with a Nikon C1 system (Nikon). The 8-OHdG-positive cells were identified by green fluorescence.

2.7 *Assessment of Spiral Ganglion Neurons*

Animals were decapitated 8 weeks after LISW exposure. These animals were transcardially perfused with a fixation solution containing 4% PFA. The entire cochleae were dissected and kept in the fixative overnight. After decalcification with 0.1 M EDTA in PBS for 10 days at 4°C, the cochleae were embedded in Tissue-Tek O.T.C. The specimens were prepared as 10-μm-thick

cryostat sections, stained with hematoxylin-eosin, and viewed under a light microscope (BX51, Olympus). To quantify the survival of SGNs in the basal turns, the total number of SGNs was counted per 10,000 μm^2. Counts were obtained from five cochleae. For each condition, the SGN counts were obtained from three locations in the basal turn of each cochlea.

2.8 *Data Analysis*

All data values are presented as means ± SE. The ABR thresholds and percentages of missing OHCs were evaluated using the nonparametric Dunnett's test. *P*-value less than 0.05 was considered significant.

3 Results

3.1 *Histopathological Analysis*

To investigate the direct mechanical cochlear damage caused by a single LISW, the rats in Group 3 (6.1 J/cm^2) were subjected to a histopathological study immediately after LISW exposure by using hematoxylineosin staining. Immediately after LISW exposure, the tympanic membrane (TM) was not perforated in any of the dissected rats. Furthermore, mechanical damage was not observed in the organ of Corti, RW, or OW immediately after LISW exposure, as shown in Fig. 3. In addition, the Reissner's and basilar membranes contained no ruptures, the tectorial membrane was not elevated from the hair cells, and there was no obvious hemorrhaging after LISW exposure. Thus, evidence of gross cochlear trauma was not detected.

3.2 *Auditory Brainstem Response*

The time courses for the thresholds before and after LISW exposure are shown in Fig. 4. The ABR thresholds before LISW exposure were essentially equivalent in all the studied ears. Immediately after LISW exposure, no significant difference was observed in the thresholds of each group. However, higher threshold levels were obtained for the high-frequency range compared with the low-frequency range in all groups. One week after LISW exposure, the ABR thresholds were significantly different between Group 1 and Group 3 at 32 kHz ($*P < 0.05$). Two weeks after LISW exposure, significant differences were observed between Group 1 and Group 3 at 32 kHz ($*P < 0.05$). Three weeks after LISW exposure, significant differences were measured between Group 1 and Group 3 at 16, 20, and 32 kHz ($*P < 0.05$). Four weeks after LISW exposure, significant differences were detected between Group 1 and Group 3 at 16, 20, and 32 kHz ($*P < 0.05$). These results indicate a dose-dependent relationship between the overpressure of SWs and the level of hearing loss, especially in the high-frequency range.

3.3 *Hair Cell Count*

Missing OHCs were counted in F-actin-labeled surface preparations, as shown in Fig. 5(a), and the percent of OHCs loss for each group is shown in Fig. 5(b). The average OHC losses of the basal turns in Group 1, Group 2, and Group 3 were 5.6%, 16.1%, and 33.4%, respectively. The OHC losses were significantly less in the basal turns of Group 1 compared with Group 3 ($*P < 0.05$). The average OHC losses of the middle turns in Group 1, Group 2, and Group 3 were 3.8%, 5.8%, and 11.3%, respectively. No significant differences were observed among the groups. The average OHC losses of the apical turns in Group 1, Group 2, and Group 3 were 4.8%, 7.7%, and 11.9%, respectively. No significant differences were observed among the groups. These data indicate that the loss of OHCs induced by LISW exposure mainly occurred in the basal turn.

3.4 *8-OHdG Immunohistochemistry*

The marker 8-OHdG was used as an indicator of free radical formation. The expression of 8-OHdG was observed in the cochleae of four rats: two animals exposed to a single LISW (6.1 J/cm^2) and two animals without LISW exposure. Anti-8-OHdG staining was conducted using green fluorescence, nuclei were counterstained in blue with DAPI, and OHCs were labeled in red with F-actin. In the OHCs, immunoreactivity for 8-OHdG in the nuclei was observed at 6 h after LISW exposure, as shown in Fig. 6. Strong immunoreactivity was observed at 6 h after LISW exposure. In contrast, significantly less immunoreactivity was observed in the normal group compared with the LISW exposure group. These results indicate that the free radicals play an important role in the mechanism of LISW-induced hair cell damage.

3.5 *Quantitative Assessment of Spiral Ganglion Neurons*

The qualitative morphology of SGNs was examined in midmodiolar sections to determine the influence of LISW on SGN

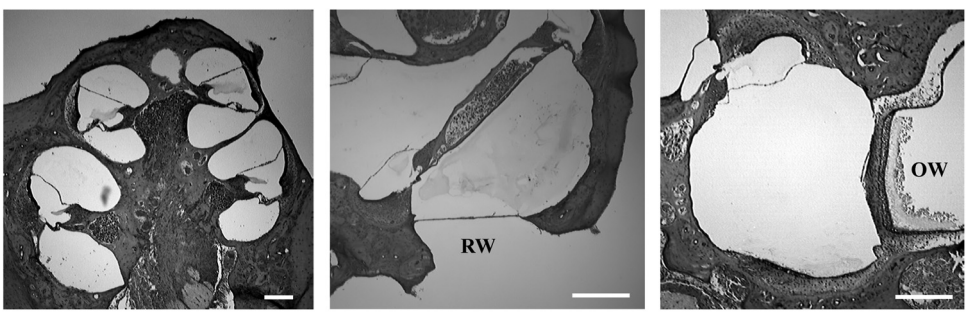

Fig. 3 (a) Whole cochlea, (b) RW, (c) and OW sections taken immediately after exposure to an LISW (6.1 J/cm^2). Mechanical damage to the cochlea, RW, and OW was not observed immediately after LISW exposure. Obvious hemorrhaging was not observed in the cochlea. Scale bar = 100 μm. RW, round window; OW, oval window.

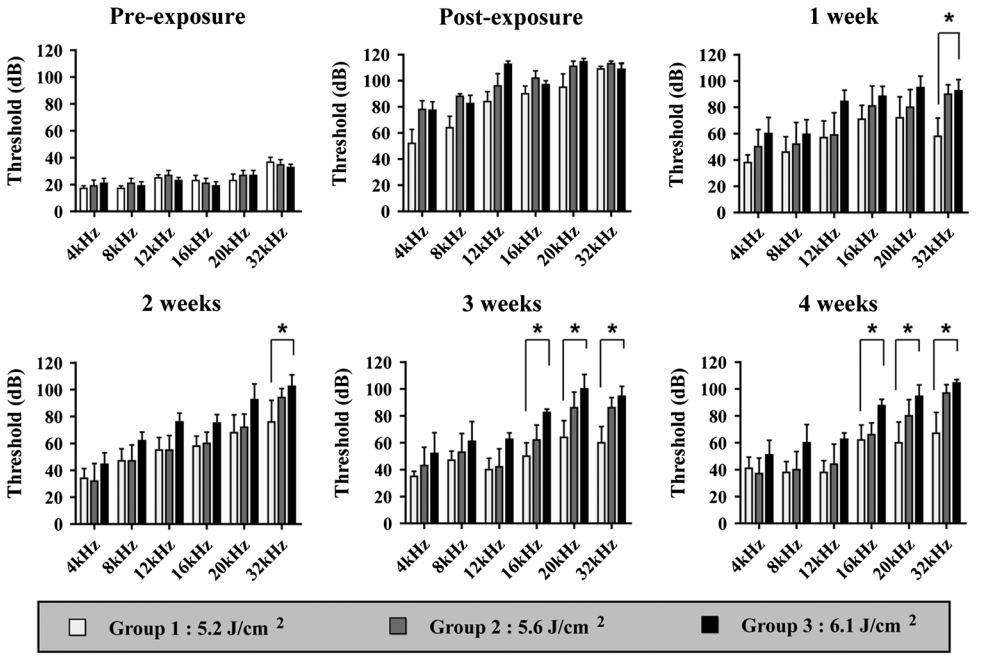

Fig. 4 Thresholds of auditory brainstem response (ABR) (mean + SE) measured before and immediately after a single LISW exposure and at 1, 2, 3, and 4 weeks after LISW exposure in Group 1 (5.2 J/cm^2), Group 2 (5.6 J/cm^2), and Group 3 (6.1 J/cm^2). The ABR thresholds had a dose-dependent relationship with the overpressure of a single LISW, with the differences becoming statistically significant at 1 week after LISW exposure (*$P < 0.05$). All statistical comparisons were conducted using the nonparametric Dunnett's test.

survival. The population of SGNs in the basal turn at 8 weeks after LISW exposure noticeably declined with increasing peak pressure, as shown in Fig. 7(a). As indicated by quantitative analysis, the survival of SGNs in the basal turn significantly decreased with increasing peak pressure, as shown in Fig. 7(b).

4 Discussion

In this study, we examined a novel animal model of SW-induced inner ear injury by using LISW. After the application of a single LISW to the cochlea, ABR measurements revealed that the rats possessed inner ear dysfunction, which was correlated with increasing LISW overpressure. Moreover, significantly lower survival rates of OHCs and SGNs, as well as severe oxidative DNA damage, were observed in the inner ear exposed to LISW. We confirmed that the application of an LISW to the cochlea causes reproducible pathologic and physiologic damages to the inner ear of rats. For this model, we applied an LISW to the cochlea through the postauricular temporal bone, rather than via EAC. Through the selected method, an SW was expected to be transmitted to the inner ear through bone conduction, creating a model with pure inner ear damage that was absent of TM perforation and with ossicular chain discontinuation. Since the SW component is considered to play an important role in blast injuries, we suggest that our LISW-based model would be useful toward elucidating the mechanisms of blast-induced inner ear injury.

Blast injuries are categorized into four phases according to the physical aspects of the blast phenomenon.[6] The primary injury phase results from physical forces emanating from the explosion and the rapid transmission of the pressure wave as an SW. The secondary injury phase typically results from debris being propelled by the blast force. The tertiary injury phase results from head contact/acceleration forces as the body is moved by the blast wind. The quaternary injury phase incorporates any injury to the brain that is not covered by the preceding three phases such as hemorrhagic shock and chemical or thermal burns.[7] Out of these four blast injury phases, the primary injury phase is the most noticeable in tissues with markedly tissue density changes such as tissueair junctions.[8] Therefore, the vast majority of blast-induced inner ear injuries may arise from an SW during the primary phase.

Reported blast pressuretime history recordings vary in the rise time of pressure, the magnitude of pressure peak, and the duration of peak overpressure and trailing underpressure before returning to ambient pressure.[9] However, it is necessary to validate the extent to which LISWs are similar to actual explosions for use as a proxy to investigate blast injuries. The peak pressure and duration of medically relevant actual explosions range from 100 kPa to 1 MPa and 0.1 to 10 ms, respectively.[10] These peak pressure ranges are roughly three orders of magnitude lower than those of LISWs, while the durations are three orders of magnitude longer.[5] However, we found that the impulse (time-integrated positive pressures) of the LISWs used in this study was in the same order of magnitude with that of medically relevant actual explosions. Because the impulse is one of the primary factors that determines the degree of pressure-induced inner ear damage,[11] we believe that the LISWs may be used to simulate part of the blast-induced inner ear injury. Furthermore, the frequency response of the LISWs used in this study was extended to 10 MHz, which is two orders of magnitude higher than the range of rodent hearing. If necessary, however, the temporal and frequency characteristics of an LISW (pressure waveform and duration) can be modified by the insertion of various materials between the bottom surface of the laser target and the tissue surface.

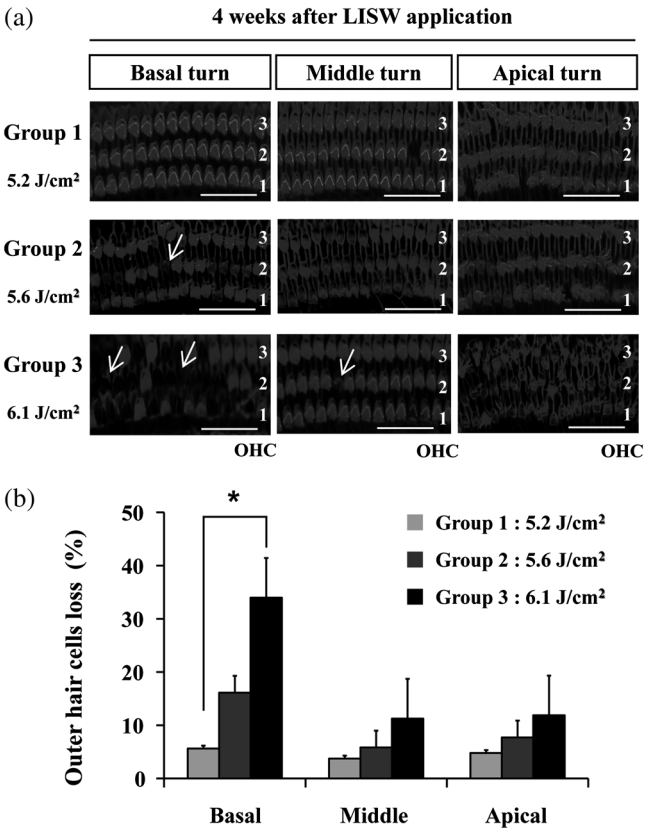

Fig. 5 (a) OHCs stained for F-actin 4 weeks after exposure to a single LISW. Less OHC death was observed in Group 1 compared with Group 3. Most LISW-induced OHC losses occurred in the basal turn compared with the apical turn. (b) The percentage of OHC loss at 4 weeks after LISW exposure. Significantly less OHC loss was observed in the basal turns of Group 1 compared with those of Group 3 ($*P < 0.05$). No significant differences were observed among the three groups for the middle and apical turns. Bars represent the standard errors (SEs) of the means. Statistical comparisons were conducted by the nonparametric Dunnett's test.

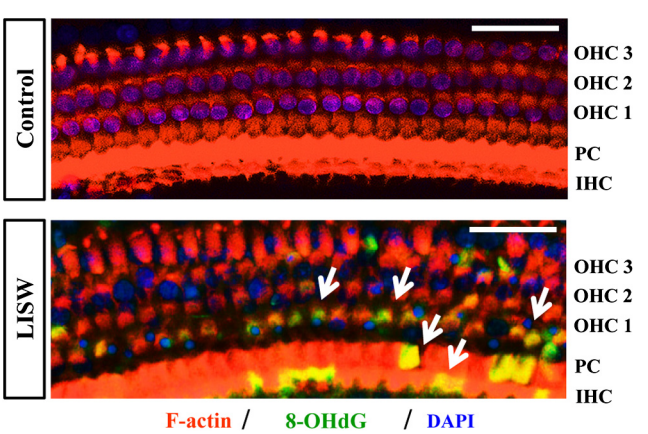

Fig. 6 Immunoreactivity of 8-OHdG in the organ of Corti. The three OHC rows are indicated by the numbers 1, 2, and 3. F-actin (red), 8-OHdG (green), and DAPI (blue). Strong immunoreactivity for 8-OHdG was observed in the LISW exposure groups. Scale bar = 50 μm. OHC, outer hair cell; IHC, inner hair cell; PC, pillar cell.

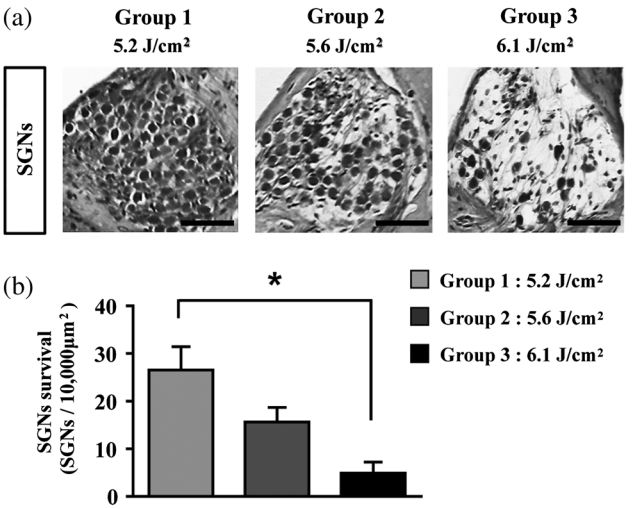

Fig. 7 (a) Spiral ganglion sections from the basal turns of each group at 8 weeks after a single LISW. A progressive loss of SGNs with increasing peak pressure was observed at 8 weeks after LISW exposure. Scale bar = 50 μm. (b) Quantitative analyses of the survival of SGNs in the basal turns. SGN survival significantly decreased with increasing peak pressure ($*P < 0.05$). Bars represent the SEs of the means. Statistical comparisons were conducted using the nonparametric Dunnett's test.

We observed a laser fluence-dependent and, hence, overpressure-dependent, level of hearing loss, as evidenced by the ABR thresholds at 4 weeks after LISW exposure. These findings support data collected from human studies following blast exposure. For example, it has been reported that the blast exposure typically results in high-frequency hearing loss.[12] In addition, our findings regarding OHC and SGN loss in the cochlea are similar to the results of previous studies describing blast-induced hearing loss.[13] Furthermore, these characteristics of LISW-induced hearing loss are also similar to those of impulse noise-induced hearing loss.[14]

Blast-induced or noise-induced cochlear damage has been attributed to two basic factors: direct mechanical stress and secondary metabolic disruption.[15] Direct mechanical stress results from the physical forces of blast-induced SWs. Further metabolic disruption is initiated during the course of blast exposure and continues to develop days or even weeks after the termination of blast exposure. The mechanisms of metabolic disruption have been linked to metabolic exhaustion via oxidative stress.[16] Lipid peroxidation, which is a consequence of oxidative stress, causes the plasma membrane to malfunction including membrane permeabilization. Depending on the level of damage, structural change to the cochlea may be either reversible or irreversible. A mild structural defect only results in a temporary threshold shift, whereas severe structural damage causes permanent defects or even hair cell death, leading to permanent hearing loss. In this study, we observed that increasing oxidative stress was associated with LISW-induced hearing impairment.

The SW-induced inner ear injury model described in the present study appears to meet the criteria established for good trauma models:[17] (1) the mechanical force (blast) is controlled, reproducible, and quantifiable; (2) the injury, as measured by ABR thresholds and cochlear hair cell loss, is reproducible under controlled and quantifiable conditions; and (3) the physical properties of the blast (amplitude and number of blast exposures) correlated with the severity and the nature of injury. The

results obtained in this study indicate that the present animal model is appropriate for investigating the mechanisms underlying SW-induced hearing loss, demonstrating the potential of using LISWs for understanding the mechanisms of blast-induced inner ear injury.

5 Conclusions

Here, we developed a method to apply LISWs to the cochlea, which could be used to create a new animal model of SW-induced inner ear injury. The model indicated that the functional and morphological changes to the inner ear of rats exposed to LISWs are similar to blast-induced inner ear injury. Although LISWs do not simulate the pressure characteristics of real blast waves, this novel rat model of SW-induced inner ear injury could prove useful for detailed laboratory studies of blast injury to the inner ear.

Acknowledgments

This work was in part supported by JSPS KAKENHI Grant Number 23592504.

References

1. A. G. Doukas and N. Kollias, "Transdermal drug delivery with a pressure wave," *Adv. Drug Delivery Rev.* **56**, 559–579 (2004).
2. Y. Satoh et al., "Targeted DNA transfection into the mouse central nervous system using laser-induced stress waves," *J. Biomed. Opt.* **10**, 060501 (2005).
3. M. Ogura et al., "In vivo targeted gene transfer in skin by the use of laser-induced stress waves," *Lasers Surg. Med.* **34**, 242–248 (2004).
4. Y. Satoh et al., "Pulmonary blast injury in mice: a novel model for studying blast injury in the laboratory using laser-induced stress waves," *Lasers Surg. Med.* **42**, 313–318 (2010).
5. S. Sato et al., "Real-time optical diagnosis of the rat brain exposed to a laser-induced shock wave: observation of spreading depolarization, vasoconstriction and hypoxemia-oligemia," *PLoS One* **9**, e82891 (2014).
6. Centers for Disease Control, and Prevention, *Explosions and Blast Injuries: A Primer for Clinicians*, CDC, Atlanta, Georgia (2006).
7. Y. C. Chen, D. H. Smith, and D. F. Meaney, "In-vitro approaches for studying blast-induced traumatic brain injury," *J. Neurotrauma* **26**, 861–876 (2009).
8. J. Garner and S. J. Brett, "Mechanisms of injury by explosive devises," *Anesthesiol. Clin.* **25**, 147–160 (2007).
9. G. Ling et al., "Explosive blast neurotrauma," *J. Neurotrauma* **26**, 815–825 (2009).
10. M. W. Courtney and A. C. Courtney, "Working toward exposure thresholds for blast-induced traumatic brain injury: thoracic and acceleration mechanisms," *Neuroimage* **54**, S55–S61 (2011).
11. R. N. Schumacher and B. E. Cummings, "A modified pressure-impulse blast damage model," USA Ballistic Research Laboratories Memorandum Report #2724, ADA036196 (1977).
12. S. A. Fausti et al., "Auditory and vestibular dysfunction associated with blast-related traumatic brain injury," *J. Rehabil. Res. Dev.* **46**, 797–810 (2009).
13. S. Cho et al., "Mechanisms of hearing loss after blast injury to the ear," *PLoS One* **8**, e67618 (2013).
14. R. Kopke et al., "Prevention of impulse noise-induced hearing loss with antioxidants," *Acta Oto-Laryngol.* **125**, 235–243 (2005).
15. M. E. Hoffer and C. D. Balaban, "Neurotologic consequences of blast injury," *NeuroTrauma Lett.* (2010). http://www.internationalbrain.org/articles/neurotologic-consequences-of-blast-injury/.
16. D. L. Ewert et al., "Antioxidant treatment reduces blast-induced cochlear damage and hearing loss," *Hear. Res.* **285**, 29–39 (2012).
17. I. Cernak and L. J. Noble-Haeusslein, "Traumatic brain injury: an overview of pathobiology with emphasis on military populations," *J. Cereb. Blood Flow Metab.* **30**, 255–266 (2009).

Biographies of the authors are not available.